UNIVERSITY OF BRISTOL

Peer reviewed version

University of Bristol - Explore Bristol Research
General rights

Mapping the contact area of the patellofemoral joint: the relationship between stability and congruence

AUTHORS:

Damian Clark [1], Jarrad M Stevens [1], Domingo Tortonese [2], Michael R. Whitehouse[1,3,4], Danielle Simpson [5], Jonathan Eldridge[1],

INSTITUTION:

1: Avon Orthopaedic Centre, Southmead Hospital Bristol, UK

2: Centre for applied anatomy, Univeristy of Bristol, UK

3: Musculoskeletal Research Unit, Translational Health Sciences, Bristol Medical School, 1st Floor Learning & Research Building, Southmead Hospital, Bristol, BS10 5NB

4: National Institute for Health Research Bristol Biomedical Research Centre, University Hospitals Bristol NHS Foundation Trust and University of Bristol

5: University of Nottingham Medical School

Damian Clark MBBS, FRCS, MSc

Jarrad Stevens, MBBS, ChM, FRACS, FAOrthA

Domingo Tortonese, D.V.M, PhD

Michael R Whitehouse PhD, MSc, BSc, MB ChB, FRCS(T&O), PG Cert(HE), FHEA

Danielle Simpson, BSc

Jonathan Eldridge, MBChB, BSc, FRCS, FRCS(T&O)

CORRESPONDENCE: drjarradstevens@hotmail.com

32 **Abstract:**

33

34 **Aims:** (1) To determine and contrast the congruency through articular contact area of

35 the patellofemoral joint during both active and passive movement of the knee with the

36 use of an MRI control mapping technique. (2) Using the same method, to compare joint

37 congruency for stable and unstable patellofemoral joints.

38

39 **Method:** A prospective case-control MRI imaging study of patients with a history of

40 patellofemoral joint instability and volunteers with no knee symptoms was performed.

41 The patellofemoral joints were imaged with the use of an MRI scan during both passive

42 and active movement from 0 through to 40 degrees of flexion. The congruency through

43 contact surface area was mapped in 5mm intervals on axial slices.

44

45 **Results:** Forty people took part in this study. The cases group included 31 patients

46 who had symptomatic patellofemoral instability and the control group included nine

47 asymptomatic volunteers. The unstable patellofemoral joints were demonstrably less

48 congruent than the stable patellofemoral joints throughout the range of knee movement.

49 The greatest mean differences between unstable and stable patellofemoral joint

50 congruency were observed between 11 and 20 degrees flexion ($1.73cm^2$ vs $4.00cm^2$,

51 $p<0.005$).

52

53 **Conclusion:** The congruency within the two groups for active and passive range of

54 movement is closely correlated. The unstable patellofemoral joint is less congruent than

55 the stable patellofemoral joint throughout knee movement. This approach to mapping

56 patellofemoral joint congruency may aid in the design of operations to increase stability

57 and serve to assess pre- and post-operative interventions as a measurable outcome.

58

59 **Introduction**

60

61 The patellofemoral joint (PFJ) is geometrically complex, asymmetric and heavily

62 influenced by kinematic forces about the knee. Patella engagement and subsequent

63 congruence of the patella in the trochlear groove provides stability and dispersion of

64 forces across the articulating surfaces with conformity of shape and movement.

65   In 1976, Goodfellow described changes in contact area that occur in the normal

66 knee with the distal patella engaging in extension while the proximal patella articulated

67 in flexion [1]. In the unstable joint, the patella will articulate in an abnormal manner to

68 produce uneven distribution of forces presenting as subluxation and even dislocation of

69 the patella. Incongruency of the patellofemoral joint, even without patella dislocation,

70 leads to degenerative changes [2-7].

71   Visualising the congruency of the PFJ through imaging modalities is useful for

72 establishing diagnosis, planning operative intervention and evaluating post-operative

73 intervention [8]. Methods for assessing the PFJ include plain radiographs, ultrasound

74 scan, computerised tomography (CT), magnetic resonance imaging (MRI) and three-

75 dimensional computer navigation [8-12]. Accurate assessment of the congruency of the

76 PFJ is vital in understanding the relationship of the bone and cartilage architecture,

77 vectors about the joint and soft tissue restraints.

78   In order to improve objective MRI analysis of the unstable PFJ, we sought to

79 map contact area through a range of passive and quadriceps active movement. Although

80 this technique is not designed to be utilised as a routine investigation, we have

81 undertaken this study to document quantifiable measurements of the unstable PFJ.

82 Additionally, we performed this imaging study on a control group of stable knees for a

83 comparison and documentation of normal contact area throughout range of movement.

84 Our hypothesis is that the unstable joint will be less congruent than the stable joint

85 through passive and quadriceps active range of movement when mapped on multiple

86 sequence MRI scan. With the ability to quantify congruency, the authors intend to

87 compare pre- and post-stabilisation surgery contact area utilising this same technique.

88 The clinical importance of this is demonstrated through the ability to objectively

89 measure PFJ contact area and hence compare the pre-operative unstable joint with the

90 change in contact area and perhaps the effectiveness of surgery with post-operative

91 MRI mapping. With the aid of the results from this study, researchers will be able to

92 compare surgical cases to a baseline cohort of patients with stable knees.

93   The aims of the study were: (1) To describe the articulating surface area of the

94 PFJ in both active and passive movement; (2) To compare joint contact area using this

95 method for stable and unstable patellofemoral joints.

96

97 **Material and methods**

98

99 This study has ethical approval (12/SW/0155) and all participants gave written

100 informed consent. A single centre, prospective case-control MRI imaging study of

101 patients with PFJ instability (cases n=31) and volunteers with no PFJ symptoms

102 (controls n=9) was performed. An MRI scan was used to capture the PFJ articular

103 cartilage contact area in a range of degrees of knee flexion in both quadriceps active

104 and passive positions for both cohorts. MRI was selected as it permits assessment of

105 anatomy in the axial, coronal and sagittal plan but can be oriented to any anatomical

106   axis which was needed for the dynamic assessment performed in this study. The

107   advantage over CT is that it permits more accurate assessment of congruence by

108   accounting for articular cartilage as well as bone. It is non-destructive and does not

109   involve ionising radiation and is therefore suitable for cases and controls.

110   The cohort size was based on a two sample independent t-test with a mean difference

111   of $2cm^2$ with equal standard deviation of 1.75, power of 80%, and type I error =0.05

112   with a sampling ratio of 3:1 (cases:controls) yielding a minimum required sample size

113   of 27 cases and nine controls. Our actual study size was 31 cases and nine controls.

114   Inclusion criteria for the cases cohort included patellofemoral joint instability

115   for consideration of surgical management. The diagnosis of instability was a

116   culmination of history (which included at least two prior episodes of patella

117   dislocation), examination, and imaging investigations. Inclusion into the control group

118   required volunteers who reported no symptoms currently or previously from the PFJ,

119   and demonstrated normal knee examination with no clinical signs of instability.

120   The exclusion criteria included patients who were unable to provide valid

121   consent, were unwilling to participate, aged 17 years or less, suffered degenerative knee

122   joint disease (including any evidence of osteoarthritis observed on radiographs AP,

123   lateral and skyline views), were pregnant, a history of metal objects or the possibility

124   of metal object in soft tissues, particularly brain, eye, heart, spinal cord or if they were

125   uncontactable by telephone.

126   The case subjects were recruited from the patient waiting list for surgery at a

127   tertiary elective orthopaedic unit. Ninety-one consecutive patients were considered to

128   be potentially eligible case subjects based on inclusion criteria. Of these, 72 were

129   willing to discuss the study and 39 agreed to participate. There were eight patient

130   withdrawals, leaving a cohort size of 31 (flowchart seen in Figure 1).

131   Information regarding; age, symptoms, previous dislocations, hypermobility

132   and imaging results (Tibial Tuberosity Trochlear Groove, Insall Salvati Ratio, Biedert

133   Patellotrochlear Index, Dejour grade) were obtained from patient notes and Picture

134   Archiving and Communications Systems (PACS).

135   The control group was used to define normal values and validate the study

136   methodology. Nine healthy volunteers were recruited from the hospital staff and

137   researcher group who demonstrated normal knee and no history of patellofemoral joint

138   symptoms. No formal imaging prior to the MRI scan was organised for participants in

139   the control group.

140

141   **Figure 1:** Flowchart of patient inclusion and exclusion.

142

143   **MRI Scanner:**

144   MRI was performed with a GE Discovery MR450 1.5 tesla scanner and an eight-

145   channel cardiac coil. The subject underwent a standard checklist where they were asked

146   specific questions regarding comfort and safety in the MRI scanner.

147

148   **Patient Position:**

149   The subject lay supine on the MRI table with a triangular wedge under the knee and a

150   strap over the thighs in order to maintain the position of the femur during the

151   examination (Figure 2A). Data was captured in both passive and quadriceps active

152   movement.

153

154   The initial localiser MRI sequence performed was an ultrafast gradient echo 3 plane

155   localiser. The localiser scan permitted the technician to identify the boundaries of the

156 trochlea and plan the location of the definitive scan. The scan boundaries were placed

157 beyond the boundaries of the trochlea in order to ensure full capture of the area of

158 interest. Blocks of axial images were captured with one sagittal localiser to calculate

159 the precise knee flexion position. The axial image was centred over the trochlea and

160 then as the knee extended the patella came into view, maintaining at all times the same

161 series of images of the trochlea.

162

163 **Passive movement imaging:**

164 The patient was secured as above and the knee permitted to rest at 40 degrees of flexion,

165 a series of images was captured. A further foam cushion was placed under the heel to

166 attain a scan at 20 degrees of flexion, finally a further cushion was placed to attain a

167 scan at 0 degrees of flexion and the series repeated a further time (Figure 2B). The angle

168 of flexion was recorded by means of tibiofemoral angle on the sagittal localiser image

169 as opposed to the thigh-calf angle used to position the patient.

170

171 **Quadriceps active imaging:**

172 The patient was positioned supine with a triangular foam pillow under the knee. A

173 beach ball was placed anterior to the tibia with a valve under the control of the subject

174 (Figure 3). The subject was requested to extend the knee, pushing the lower leg against

175 the balloon, causing it to deflate (Figure 2C). Subjects were advised that it would be

176 expected to take two minutes to achieve this. The MRI operator informed the subject

177 that the scan was due to start so as to coincide this with the beginning of the scan. As

178 the knee extended the scan was begun and repeated whilst the subject deflated the

179 balloon.

180

181 Rapid sequence axial images were captured whilst the ball was permitted to continue

182 to deflate under the subject's control. The deflation rate was dependent upon the

183 exertion of the patient and was not externally controlled. Five to eight sequences were

184 captured per deflation.

185

186 **Imaging sequence:**

187 After the localiser scan located the distal femur, the sequence placement was planned

188 so that the entire trochlea could be imaged. In both the active and passive modes, the

189 thigh did not move due to control by strapping and it was possible to attain adequate

190 quality imaging of the trochlea, without motion artefact. In each sequence, images

191 captured included one sagittal slice and 10-18 axial slices (dependent on patient size)

192 at 5mm intervals.

193

194 In any given scan, up to 5 images demonstrated contact between the patella and the

195 trochlea and at any given moment, the entire trochlea was captured in order to ensure

196 all the relevant images along the path of the patella were captured.

197

198 **Image interpretation:**

199

200 Using digital data supplied by the institutional PACS (GE Healthcare Centricity™ &

201 Fujifilm Synapse™) the operator manually identified boundaries of cartilage contact

202 between the patella and femur on both sides of the trochlear sulcus on the axial view.

203 These measurements were recorded as linear distances. Each slice is 5mm wide and the

204 surface area of each slice was calculated by multiplying the length by 5mm. Each slice

205 surface is then summed to reach a measure of the surface area in contact between the

206   articulating surfaces to give a measure of congruency in each measurement condition.

207   This was recorded on a "flattened" 2D coronal plane image for visual interpretation of

208   contact area (Figure 4).

209

210   Statistical methods:

211   The repeatability of the measurements of MRI congruity were assessed by

212   Pearson's correlation coefficient. The measurements were repeated by the primary

213   investigator at a second timepoint to give a measure of intra-observer error. The

214   measurements were repeated by another observer for assessment of inter-observer

215   error. Comparison between case and control variables was made with a Fisher's exact

216   test or Chi^2 test for categorical variables depending upon number of groups or

217   independent t-tests for continuous data. Two-tailed independent sample t-tests were

218   used to compare the mean joint congruence (cm^2) between cases and controls during

219   the different phases of knee flexion during quadriceps activation (0 degrees, 0-10, 11-

220   20, 21-30, 31-40, >40 and combined). All statistical analyses were performed using

221   SPSS (IBM SPSS Statistics, Armonk, NY, USA).

222

223   **Results:**

224

225   Between the cases and controls, the ages were well balanced. The mean age was

226   25 (range: 16-42; SD 6.9) in the case group and 26 (range: 19-32; SD 5.1) in the controls

227   (p=0.690; Table 1). There were 19 females and 12 males in the cases group (p=0.060;

228   Table 2). Laterality (side studied) was also well balanced, 36% being left amongst the

229   cases and 44% amongst the controls (p=0.705). The other co-variates of interest that

230   are associated with the pathology were more frequent amongst the cases than the

231   controls (Table 2). All patients in the cases group had sustained at least 2 dislocations

232   with 19 (61%) sustaining more than 2 dislocations. Seven (22.6%) of the cases cohort

233   have hypermobility with a Beighton score of four or more. Only six (19%) patients in

234   the cases cohort demonstrated a normal trochlear groove with the 14 patients (45%)

235   displaying Dejour C abnormalities. Unsurprisingly, all control group patients

236   demonstrated a normal trochlear groove.

237   The radiological measurements were highly correlated for intra-observer error

238   (0.985) and for inter-observer error (0.910). The congruency within the two groups for

239   active and passive range of movement is closely correlated (Figure 5). The histogram

240   illustrates the trend from incongruence to congruency as the knee flexes (Figure 6). The

241   greatest differences in congruency between controls and cases is seen in the quadriceps

242   active group between the range of zero and twenty degrees. The greatest mean

243   differences and greatest statistical significance is at the 11-20 degree range (Figure 6).

244   The curves match well between controls and cases; the exception is at the 40+ range

245   where there only one case has been recorded and the trend for increased congruence is

246   not observed.

247

248   **Discussion:**

249   The clinical importance of this study is to establish a direct measurement of PFJ

250   contact area. With the ability to quantify congruency, the authors intend to use this

251   technique to compare pre-operative and post-operative in cases where stabalisation

252   surgery is performed.

253   With the aid of the results from this study, researchers will be able to compare

254   surgical cases to a baseline cohort of patients with stable knees. The range 11-20

255　degrees (tibiofemoral angle) is the most sensitive. Clinicians may use the routine MRI

256　performed in this position to evaluate congruence by this technique.

257　　　　　The PFJ is a complex articulation for which accurate assessment of congruence

258　and morphology may remain elusive with a single imaging modality or if viewed in a

259　single plane [13,14]. Our sequential MRI scans during active and passive range of

260　movement of the knees demonstrated close correlation of contact area within the groups

261　for both active and passive range of movement. When the control and cases groups are

262　compared, the mean contact area was greater in the control group through all ranges of

263　movement in both passive and quadriceps active with the exception of quadriceps active

264　in extension. This may be secondary to an abnormal articulation of the unstable patella

265　within the trochlear by activation of the quadriceps in this position.

266　　　　　The greatest mean differences between unstable and stable patellofemoral joint

267　congruency during quadriceps active series were observed between 11 and 20 degrees

268　($1.73cm^2$ vs $4.00cm^2$, p<0.001). This is important as lateral patellar displacement has

269　been shown to occur with the lowest restraining forces required at 20 degrees of knee

270　flexion [15].

271　　　　　Understanding articular contact through imaging modalities is problematic with

272　significant mismatch between osseous landmarks observed in radiographs or CT scans

273　and the articular cartilage of the patella and trochlea obtained by an MRI [16]. Patella

274　position has been evaluated with the use of many different indexes, such as the Insall-

275　Salvati [17], the modified Insall-Salvati [18] the Blackburne-Peel [19], the Caton-

276　Deschamps [20] and the Sagittal Patellofemoral Engagement (SPE) Index [21].

277　Radiographic classifications have been also reproduced with MRI [22]. Whilst patella

278　height and engagement can be assessed in the sagittal plane, an appreciation of

279　congruency especially through range of movement is not achieved.

280 Axial imaging provides information on the position of the patella within the

281 trochlear groove, however, static knee position images provide little information

282 toward the congruency or tracking through the range of movement. Skyline plain

283 radiographs have been found to be unreliable [23,24], because they can be difficult to

284 obtain at degrees of flexion less than 30 where subluxation is most prevalent. It is for

285 these reasons we sought to evaluate the patellofemoral joint by means of contact area

286 through axial MRI imaging during active movement as cartilage contact is the

287 functional basis of force transmission. Several other authors have previously given

288 attention to activation of the quadriceps mechanism during capture of axial imaging

289 [24-26].

290 Brossmann et al. used dynamic MRI to analyse patella tracking in healthy

291 volunteers and patients with maltracking [25]. They reported significantly different

292 patellar tracking patterns between the two groups and statistically significant tracking

293 differences between static and dynamic scanning of the PFJ although the contact

294 surface area was not a measured outcome. While McNally et al. described the

295 morphological traits of instability with dynamic axial MRI there was no recording of

296 congruency or contact area [26]. They demonstrated with the use of dynamic MRI that

297 patella subluxation was present in 40% of patients with anterior knee pain and

298 challenged the clinical relevance of mild subluxation of the PFJ. Martinez et al. utilised

299 CT scans at set intervals of 0, 20 and 45 degrees of flexion to establish the effect of

300 activation of the quadriceps on the centralisation and tilt of the patella [27]. The

301 individuals assessed had asymptomatic knees and were considered healthy. They

302 concluded that Quadriceps contraction had little influence on the patellar centralisation

303 and did not effect patellar tilt unless in full extension. The effect on unstable PFJs was

304 not explored by these authors.

305   We have sought to quantify the congruency of the PFJ through dynamic MRI

306   mapping and 2D representation of contact surface area. We have documented the

307   difference in contact surface area between the stable and unstable PFJ. The potential to

308   use this MRI mapping methodology to establish the change in congruency for pre- and

309   post-stabilisation surgeries will allow for objective evaluation of treatment modalities.

310   Despite the small sample size of this study there were significant differences in

311   the contact area at all ranges between 0 and 40 degrees when comparing cases and

312   controls. The gender imbalance of male n=7 to female n=2 in the control group is seen

313   by the authors as a weakness of the study as the majority of PFJ instability cases are

314   seen in the female population. The disadvantages of adding a dynamic element to MRI

315   imaging has the potential for generation of movement artefact with the addition of a

316   further variable which may increase the variance of the data. The issue of motion

317   artefact was minimal as the rapid sequence MRI scan coupled with stabilisation of the

318   femur resulted in clear and accurate images for interpretation. Despite the risk of

319   motion artefact, the authors believe dynamic imaging of the PFJ may be more

320   representative of the physiologic conditions that are present during ambulation.

321   The range of movement is limited to 40 degrees of flexion due to the physical

322   constraints of the MRI scanner.

323   The articulation of the PFJ, if accurately measured in terms of contact area, will

324   provide useful information in determining the effectiveness of surgeries aimed at

325   increasing congruency. The authors aim to compare a cohort of patients pre- and post-

326   stabilisation surgery using this methodology to quantify the effects of surgical

327   modalities on PFJ congruence.

328

329

330 **Conclusion:**

331

332 The unstable patellofemoral joint is less congruent than the stable patellofemoral joint

333 throughout knee movement. The unstable PFJ has less contact surface area and this will

334 inversely increase the contact pressure for a given force leading an increased risk of

335 degeneration of the joint. This approach to mapping of the patellofemoral joint may aid

336 in the design of operations to increase stability and serve to provide a means of

337 assessing pre- and post-operative joint congruency as an outcome measure. If a single

338 axial series is to be obtained on MRI scan, the authors recommend 10-20 degrees of

339 tibiofemoral flexion as this was shown to have the greatest difference in contact surface

340 area between the cases and controls group.

341

342

343   **Figure 1**: Flow chart of case inclusion and exclusion.

344   **Figure 2:** A: The subject lay supine on the MRI table with a triangular wedge under

345   the knee. B: Foam blocks were placed for passive range of movement at 0, 20 and 40

346   degrees flexion. C: Deflating balloon against resistance with multiple sequence scans

347   for Quadriceps active.

348   **Figure 3:** A beach ball was placed anterior to the tibia to provide resistance and achieve

349   quadriceps activation. The subject controlled a valve to control the rate of deflation.

350   **Figure 4:** "Flattening" of axial imaging. Slices are at 5mm intervals. The width of each

351   slice in which there is contact between femur and patella cartilage is multiplied by

352   5mm. Each measurement is then summed to give a total area of congruence.

353   **Figure 5:** Control vs Instability group in passive and active movement.

354   **Figure 6:** Histogram in quadriceps active, control and instability

355

356   **Table 1:** Age, Tibial Tuberosity Trochlear Groove (TTTG) distance (mm), Insall

357   Salvati Ratio (ISR), Biedert Patellotrochlear Index, SD = standard deviation, n =

358   number.

359   **Table 2:** Clinical comparison between cases and controls.

360   **Table 3:** Comparison of mean joint congruence between case and controls during

361   quadriceps active knee movement.

362

363

364   **REFERENCES:**

365

366   1: Goodfellow J, Hungerford DS, Zindel M. Patello-femoral joint mechanics and

367   pathology. 1. Functional anatomy of the patello-femoral joint. J Bone Joint Surg

368   Br. 1976 Aug;58(3):287-90.

369

370   2: Dejour H, Walch G, Neyret P, Adelein P. Dysplasia of the femoral trochlea. Rev

371   Chir Orthop 1990;76:45–54.

372

373   3: Eijkenboom JFA, Waarsing JH, Oei EHG, Bierma-Zeinstra SMA, van Middelkoop

374   M. Is patellofemoral pain a precursor to osteoarthritis? Bone Joint Res. 2018 Oct

375   3;7(9):541-547.

376

377   4: Luyck T, Didden K, Vandenneucker H, Labey L, Innocenti B, Bellemans J.

378   Is there a biomechanical explanation for anterior knee pain in patients with patella alta?

379   J Bone Joint Surg Br 2009;91-B(3):344-350.

380

381   5: Conchie H, Clark D, Andrew M, Eldridge J, Whitehouse M. Adolescent knee pain

382   and patellar dislocations are associated with patellofemoral osteoarthritis in adulthood:

383   A case control study. Knee 2016;23(4):708-711.

384

385   6: Utting MR, Davies G, Newman JH. Is anterior knee pain a predisposing factor to

386   patellofemoral osteoarthritis? Knee 2005;12(5):362–5.

387

388   7: Clark D, Metcalfe A, Wogan C, Mandalia V, Eldridge. Adolescent patellar

389   instability: current concepts review. J Bone Joint J. 2017 Feb;99-B(2):159-170.

390

391   8: Keller JM, Levine WN. Evaluation and Imaging of the Patellofemoral Joint.

392   Operative Techniques in Orthopaedics 2007;17(4):204-210.

393

394

395

396   9: Merchant AC, Mercer RL, Jacobsen RH, Cool CR. Roentgenographic analysis of

397   patellofemoral congruence. J Bone Joint Surg Am 1974;56:1391-1396 .

398

399   10: Oye CR, Holen KJ, Foss OA. Mapping of the femora trochlea in a newborn

400   population: an ultrasonographic study. Acta Radiol 2014;2:234-43.

401

402   11: Alemparte J, Ekdahl M, Burnier L, et al. Patellofemoral evaluation with

403   radiographs and computed tomography scans in 60 knees of asymptomatic subjects.

404   Arthroscopy 2007;23(2):170-177.

405

406   12: Wittstein JR, Bartlett EC, Easterbrook J, Byrd JC. Magnetic resonance imaging

407   evaluation of patellofemoral malalignment. Arthroscopy 2006;22:643-649.

408

409   11: Victor J, Van Glabbeek F, Vander Sloten J, Parizel PM, Somville J, Bellmans J. An

410   experimental model for kinematic analysis of the knee. J Bone Joint Surg Am

411   2009;91(6):150-63.

412

413   12: Hashimoto S, Ochs RL, Komiya S, Lotz M. Linkage of chondrocyte apoptosis and

414   cartilage degradation in human osteoarthritis. Arthritis Rheum 1998;41(9);1632-1638.

415

416   13:   Saggin PR, Saggin JI, Dejour D. Imaging in patellofemoral instability: an

417   abnormality-based approach. Sports Med Arthrosc 2012;20(3):145-51.

418

419   14:   Becker R, Hirschmann MT, Karlsson J. The complexity of patellofemoral

420   instability. Knee Surg Sports Traumatol Arthrosc 2018;26(3):675–676.

421

422   15: Senavongse W1, Farahmand F, Jones J, Andersen H, Bull AM, Amis AA.

423   Quantitative measurement of patellofemoral joint stability: force-displacement

424   behavior of the human patella in vitro. J Orthop Res 2003;21(5):780-6.

425

426   16: Staeubli HU, Bosshard C, Porcellini P, Rauschning W. Magnetic resonance

427   imaging for articular cartilage: cartilage-bone mismatch. Clin Sports Med

428   2002;21(3):417-33 [viii-ix].

429

430   17: Insall J, Salvati E. Patella position in the normal knee joint. Radiology

431   1971;101(1):101-104.

432

433   18: Grelsamer RP, Meadows S. The modified Insall-Salvati ratio for assessment of

434   patellar height. Clin Orthop Relat Res 1992;282:170-176.

435

436   19: Blackburne JS, Peel TE. A new method of measuring patellar height. J Bone Joint

437   Surg Br 1977;59(2):241-242.

438

439   20: Caton G, Deschamps, Chambat G, Lerat JL, Dejour H. Patella infera. Apropos of

440   128 cases. Rev Chir Orthop Reparatrice Appar Mot 1982;68(5):317-325.

441

442   21: Dejour D, Ferruaa P, Ntagiopoulos PG et al. The introduction of a new MRI index

443   to evaluate sagittal patellofemoral engagement. Orthop Traumatol Surg Res 2013;99(8

444   Suppl):S391-S398.

445

446   22: Miller TT, Staron RB, Feldman F. Patellar height on sagittal MR imaging of the

447   knee. Am J Roentgenol 1996;167(2):339-341.

448

449   23: Walker C, Cassar Pullicino VN, Vaisha R, McCall IW. The patello-femoral joint:

450   a critical appraisal of its geometric assessment utilizing conventional axial radiography

451   and computed arthro-tomography. Br J Radiol 1993;66(789):755-761.

452

453   24: Inoue M, Shino K, Hirose H, Horibe S, Ono K. Subluxation of the patella.

454   Computed tomography analysis of patellofemoral congruence. J Bone Joint Surg Am

455   1998;70(9):1331-1337.

456

457   25: Brossmann J, Muhle C, Schroder C et al. Patellar tracking patterns during active

458   and passive knee extension: evaluation with motion-triggered cine MR imaging.

459   Radiology 1993;187(1):205-212.

460

461   26: Mcnally EG, Ostlere SJ, Pal C, Phillips A, Reid H, Dodd C. Assessment of patellar

462   maltracking using combined static and dynamic MRI. Eur Radiol 2000;10(7):1051-5.
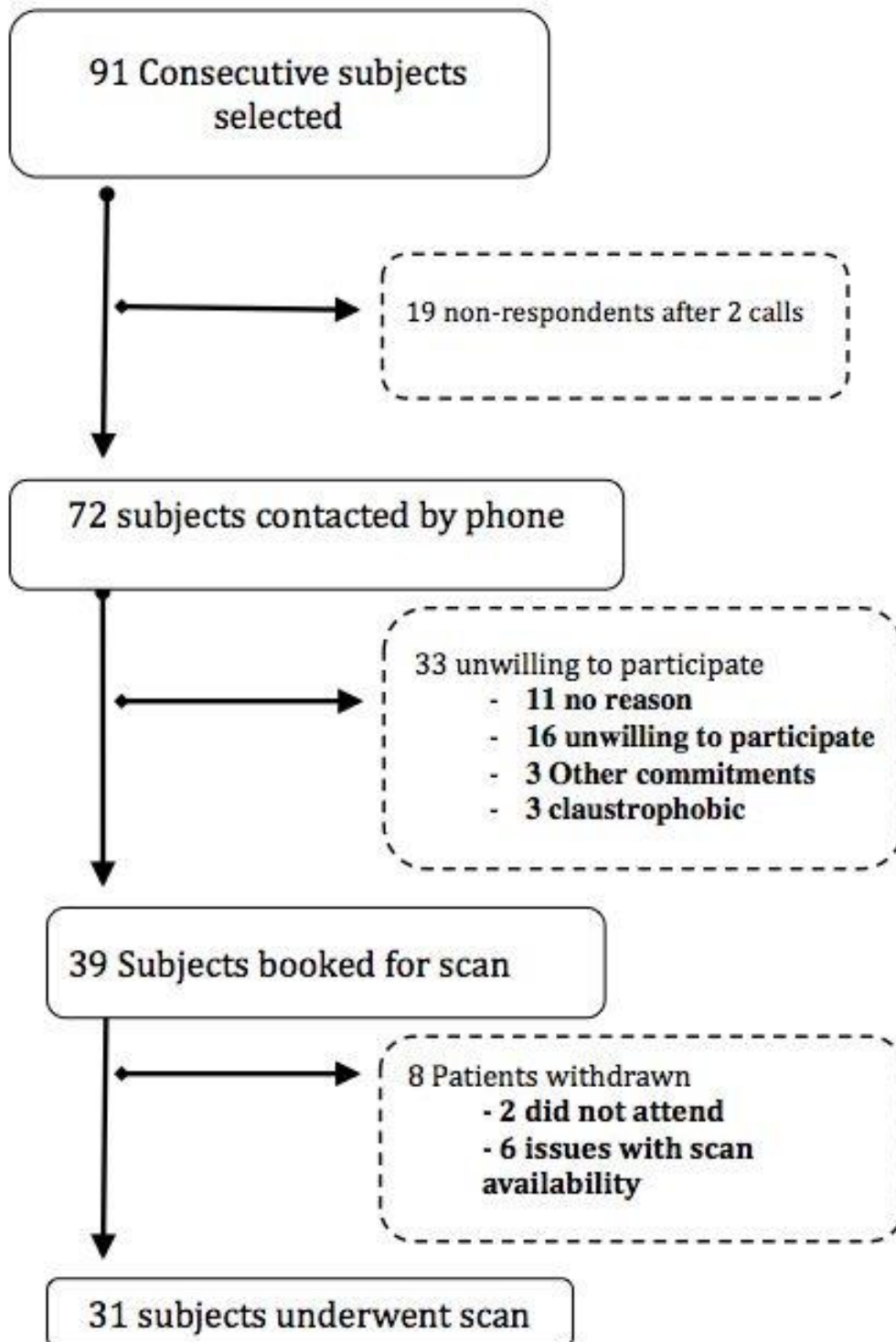
463

464   27: Martinez S, Korobkin M, Fondren FB, Hedlund, LW, Goldner JL. Computed

465   tomography of the normal patellofemoral joint. Invest Radiol 1983;18(3):249-53.
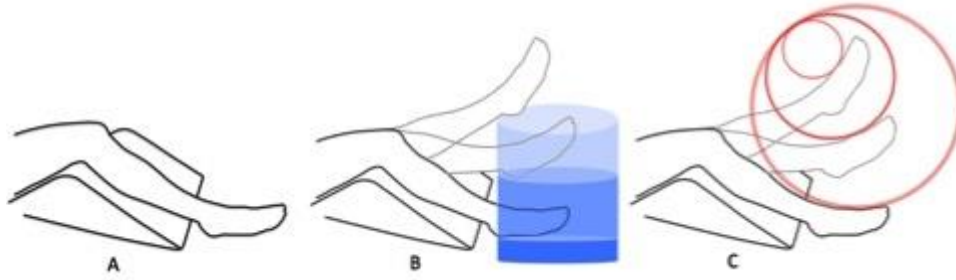
466

467 **Figure 1**: Flow chart of case inclusion and exclusion.

468

469
470

471 **Figure 2**: A: The subject lay supine on the MRI table with a triangular wedge under

472 the knee. B: Foam blocks were placed for passive range of movement at 0, 20 and 40

473 degrees flexion. C: Deflating balloon against resistance with multiple sequence scans
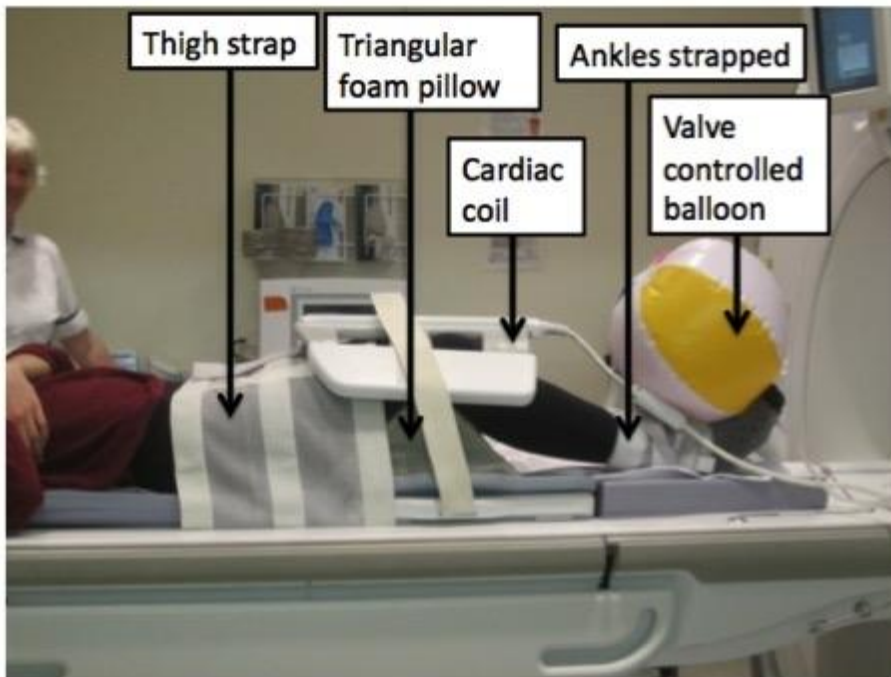
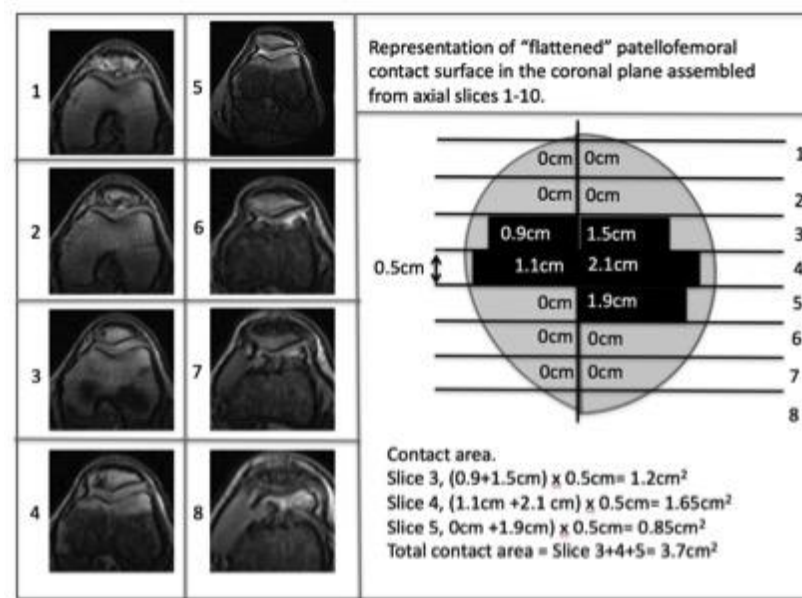474 for Quadriceps active

475
476

477

478

479 **Figure 3**: A beach ball was placed anterior to the tibia to provide resistance and achieve

480 quadriceps activation. The subject controlled a valve to control the rate of deflation.
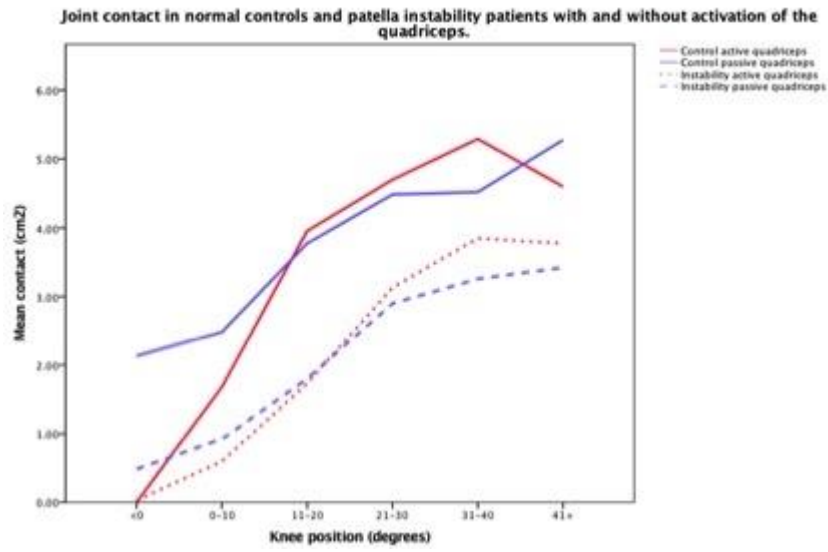

481
482

483

484   **Figure 4**: "Flattening" of axial imaging. Slices are at 5mm intervals. The width of each

485   slice in which there is contact between femur and patella cartilage is multiplied by

486   5mm. Each measurement is then summed to give a total area of congruence.

487
488

489

490 **Figure 5**: Control vs Instability group in passive and active movement.

Joint contact in normal controls and patella instability patients with and without activation of the quadriceps.

491
492

493

494   **Figure 6**: Histogram in quadriceps active, control and cases groups

Error Bars: 95% CI
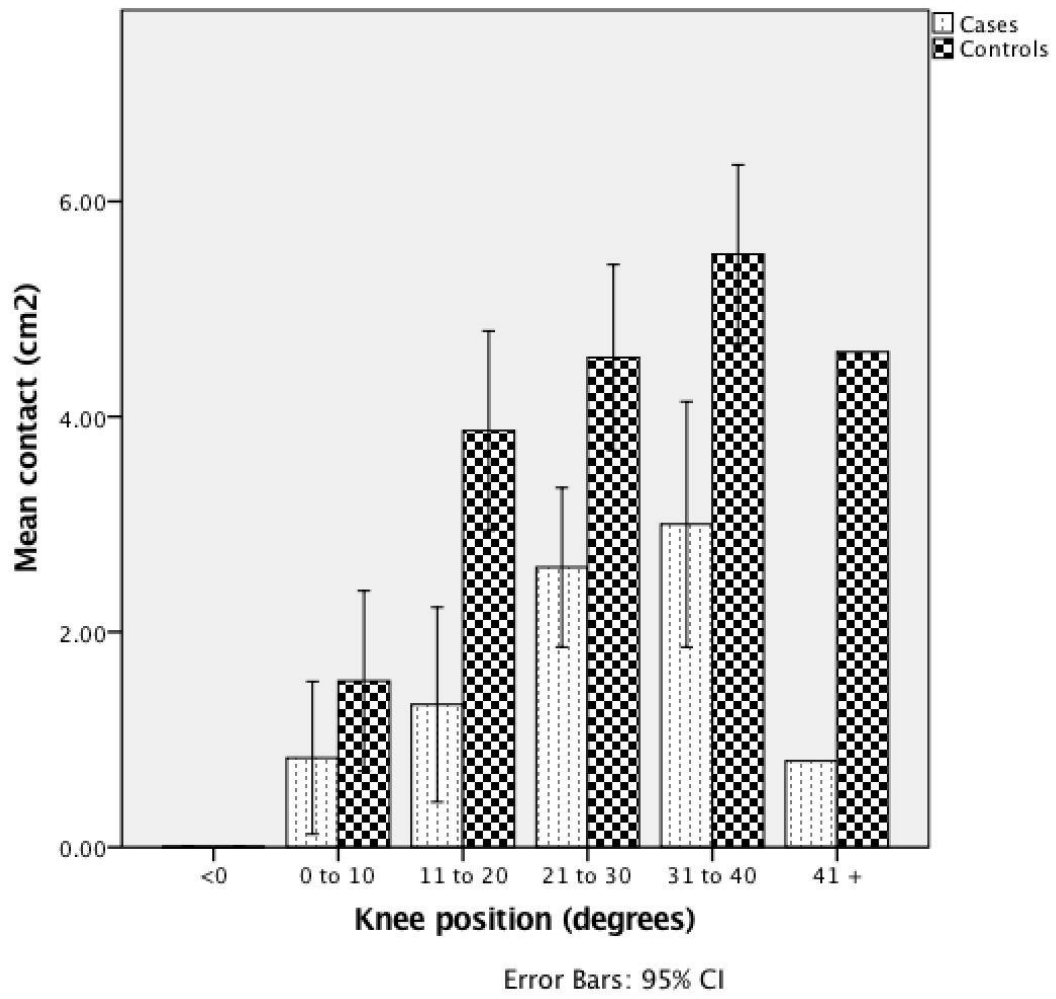
495
496

497

	Cases			Controls			
	Mean	SD	n	Mean	SD	n	p value
Age	25	6.9	31	26	5.1	9	0.690
TTTG	13.3	4.6	31	11.9	3.2	9	0.400
ISR	1.37	0.2	31	1.19	0.09	9	0.013
Biedert	32.5	23	31	38.2	3.3	9	0.470
Age at 1st dislocation	14.9	3.8	21	-	-	-	

498

499 **Table 1**: Age, Tibial Tuberosity Trochlear Groove (TTTG) distance (mm), Insall

500 Salvati Ratio (ISR), Biedert Patellotrochlear Index, SD = standard deviation, n =

501 number

502

503

		Cases		Control		
		n	%	n	%	p value
Sex (female - male)		19 - 12	61 female	2-7	22.2 female	0.060
Laterality (left - right)		11 - 20	36 left	4-5	44 left	0.705
Dejour grade	Normal A B C D	6 3 5 14 3	19 10 16 45 10	9 0 0 0 0	100 0 0 0 0	0.001
Hypermobile (Beighton Score of 4+)		7/31	22.6	0/9	0	0.175
Previous surgery		7/31	22.6	0/9	0	0.175
Subjects with >2 dislocations		19/31	61	0/9	0	0.001

504
505 **Table 2**: Clinical comparison between cases and controls
506

507

Quadriceps active: knee position.		n	Mean joint congruence cm2	mean diff	95% lower	95% upper	P
<0	Case	7	0.029	0.029	-0.10	0.16	0.626
	Control	2	0.00				
0-10	Case	26	0.59	-1.09	-1.80	-0.38	0.004
	Control	11	1.68				
11-20	Case	26	1.73	-2.22	-3.16	-1.27	0.000
	Control	9	4.00				
21-30	Case	24	3.13	-1.57	-2.64	-0.49	0.006
	Control	8	4.70				
31-40	Case	18	3.85	-1.44	2.58	-0.30	0.016
	Control	5	5.29				
40+	Case	9	3.77	-0.83	-4.51	2.85	0.618
	Control	1	4.60				
Combined	Case	110	2.17	-1.24	-1.91	-0.55	0.000
	Control	36	3.40				

508

509   **Table 3**: Comparison of mean joint congruence between case and controls during

510   quadriceps active knee movement

511

512